POTENTIAL OF LOW-COST POMEGRANATE PEELS ADSORBENT FOR DYE REMOVAL FROM WASTEWATER: A SUSTAINABLE SOLUTION FOR AGRICULTURAL WASTE VALORIZATION

AMINA BEDOUI, NOUHA SOUDANI, SAMIA BEN ALI,
ABDELMOTTALEB OUEDERNI and SOUAD SOUISSI-NAJAR

Research Laboratory of Engineering Processes and Industrial Systems,
National Engineering School of Gabes, University of Gabes, St Omar Ibn El-Khattab, 6029 Tunisia
✉ *Corresponding author: A. Bedoui, amina.bedoui@gmail.com*

Received October 14, 2025

Pomegranate peel (PGP) was valorized as a low-cost and eco-friendly biosorbent for the removal of dyes from wastewater. This study investigates the adsorption performance of unmodified PGP for the removal of Victoria Blue (VB). The biosorbent was characterized using several techniques, including BET analysis, Fourier-transform infrared spectroscopy (FTIR), and scanning electron microscopy (SEM). The point of zero charge (pH_{pzc}) and surface acidity/basicity were also evaluated using the pH equilibration method and Boehm titration, respectively. Batch adsorption experiments were conducted to evaluate the effect of key parameters such as initial dye concentration, pH, contact time, and particle size. The optimum removal efficiency was achieved at pH 6, 25 °C, particle size of 0.63 mm, and an equilibrium time of 60 minutes. The adsorption equilibrium data were fitted to the Langmuir, Freundlich, and Temkin isotherm models. Among these, the Langmuir model provided the best fit with a maximum adsorption capacity of 120.48 mg/g. Kinetic studies demonstrated that the adsorption process followed a pseudo-second-order model. Thermodynamic parameters confirmed that the biosorption was spontaneous and exothermic, with negative ΔG° and ΔH° values. These results highlight raw pomegranate peel's potential as an effective and sustainable biosorbent for wastewater treatement.

Keywords: Victoria Blue dye, pomegranate peels, wastewater, characterization, biosorption

INTRODUCTION

Agricultural waste, a by-product of farming activities, has become a significant environmental concern considering its increasing accumulation globally. The rapid growth of agricultural production and processing, driven by the demand for food, feed, and bioenergy, has led to an unprecedented generation of waste materials, including, crop residues,[1,2] husks,[3,4] stalks[5] and peels.[6,7] If not properly managed, these organic by-products contribute to various environmental issues, such as air pollution, soil degradation, and water contamination. The improper disposal of these residues – often through open burning or landfilling – releases harmful greenhouse gases, particulate matter, and toxins into the atmosphere, exacerbating climate change and posing health risks to nearby communities.[8,9] In addition, agricultural waste accumulation leads to the loss of valuable organic resources, which could otherwise be utilized to enrich the soil, produce bioenergy, or serve other beneficial purposes.

On the other hand, when properly used, agricultural waste could present an opportunity for innovative recycling and reuse, especially in environmental remediation processes. Rather than being discarded or burned, agricultural residues can be effectively repurposed as valuable raw materials for a wide range of applications. By transforming these by-products through processes such as carbonization, fermentation, or biorefining, agricultural residues can be converted into sustainable products like biochar or hydrochar,[10,11] biofuels,[4] animal feed[12] and biodegradable plastics.[13]

Nevertheless, agricultural wastes can also be effectively utilized in various applications without

the need for extensive transformation, such as for the removal of contaminants from wastewater. These organic by-products, when used in their raw or minimally processed form, can serve as low-cost, sustainable adsorbents for pollutants, including dyes[14,15] and heavy metals.[16] Agricultural residues possess inherent porous structures and active sites that make them ideal candidates for wastewater treatment. This method not only provides an efficient solution to environmental pollution, but also promotes the recycling of agricultural waste, reducing disposal-related issues while offering an eco-friendly alternative to traditional treatment methods.

Dyes are colored organic compounds, and their presence in effluents is a major environmental concern because of their harmful effects on various forms of life. The consumption of dyes in industries such as textiles, paints, leather, plastics, pharmaceuticals, and cosmetics has increased substantially, leading to long-term negative impacts on the environment.[17,18] Dyes are one of the most visible indicators of water pollution, as they impart undesirable colors to water, reducing sunlight penetration, which is essential for aquatic life.[19]

In many European countries, environmental regulations demand the decolorization of dye-containing wastewater prior to discharge.[20] However, dyes are often highly resistant to biodegradation, making biological treatments both costly and inefficient. Various physicochemical methods are employed for dye removal, including flocculation, membrane filtration, electro kinetic coagulation, electrochemical destruction, ion exchange, precipitation, ozonation, and adsorption.[21]

Among these techniques, adsorption stands out as one of the most effective methods for completely removing different types of dyes, even from dilute solutions.[21] The main advantage of adsorption is the minimal generation of toxic by-products,[22] as well as the use of low-cost materials, particularly agro-waste products, such as rice husk,[23] fruit peels, and fruit shells, including those from pine, olive, banana, and coconut.[24–27] These materials have been widely studied and found to be effective adsorbents for dye removal.

Pomegranate peels, a waste material from the pomegranate juice, wine, and tannery industries, is a promising candidate for biosorption applications. In Tunisia, pomegranate production generates substantial waste that could be efficiently utilized as a biosorbent for dye removal. However, few studies have explored the potential of pomegranate peel for this purpose. Ali *et al*.[28] investigated the removal of copper ions and Yellow 145 (3RS) dye using pomegranate peel, achieving optimal removal capacities of 209.7 mg/g for the dye and 103 mg/g for copper ions. Similarly, they studied the adsorption of methylene blue using pomegranate peel, with the Langmuir maximum monolayer adsorption capacity at 30 °C reaching 250 mg/g.[28]

To the best of our knowledge, not much research has been done on the biosorption of Victoria Blue dye using pomegranate peel. As a result, this study offers a fresh method for the valorization of Tunisian pomegranate peel as an efficient biosorbent for removing Victoria Blue from aqueous solutions.

The biosorption properties of natural pomegranate peel (PGP) for the removal of Victoria Blue (VB) dye from aqueous solutions was explored, without any pre-treatment applied to the PGP. The temperature used for washing and drying was kept below 50 °C. The physical and chemical characteristics of the adsorbent, including the point of zero charge (pH_{pzc}), surface functional groups, N_2 adsorption, and SEM analysis were analyzed. Additionally, the effects of solution pH, contact time, temperature, and initial dye concentration on the biosorption of VB were investigated. The experimental data were evaluated and fitted to adsorption equilibrium isotherms, kinetic models, and thermodynamic studies.

EXPERIMENTAL

Chemicals

Victoria Blue (VB), a cationic (basic) dye (Fig. 1), was chosen for this study due to its widespread use in the textile and printing industries and its frequent presence in industrial effluents. VB is known for its high stability and persistence in aquatic environments, as well as its potential toxicity to aquatic organisms and possible adverse effects on human health, making its removal from wastewater a major environmental concern.[29] The dye used in this work was supplied by Labosi, with a purity of 99.99%. Its empirical chemical formula is $C_{33}H_{32}N_3Cl$ and its molar mass is 506.08 g/mol.

A stock solution (1 g/L) was prepared by dissolving the appropriate mass of VB in one liter of distilled water. Working solutions were obtained by successive dilutions to the desired concentrations.

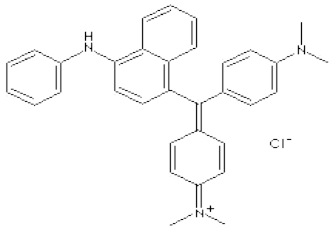

Figure 1: Molecular structure of Victoria Blue (VB)

The pH of the solutions was adjusted using 0.01 M NaOH or HCl. Dye concentrations were determined using a UV-Visible spectrophotometer (PerkinElmer) at a wavelength of 615 nm, based on a previously established calibration curve.

Preparation and characterization of the biosorbent

Pomegranate peels were collected in the southern part of Tunisia (Gabès) and thoroughly washed with preheated double distilled water to remove dust and any unwanted particles. After that, they were dried in an air oven at 50 °C overnight, ground with a ceramic mortar and sieved to the required particle size. The precursor was stored in desiccators and used without any pretreatment for VB adsorption.

Nitrogen adsorption-desorption

The textural characteristics of the PGP were determined by N_2 using an ASAP 2020 Micrometrics. Preceding each analysis, the sample was degassed at 403 K for 15 h to obtain a residual pressure of less than 10^{-5} Torr. One hour of equilibrium time was allowed for each point of N_2 adsorption. Nitrogen adsorption was carried out in a volumetric system at 77 K. The Brauner-Emmett and Teller (BET) method was used to determine the surface area available to N_2.[30]

Surface morphology

Scanning electron microscopy was used to assess the surface morphology of the precursor (SEM, Quanta 3D FEG, FEI). In order to prevent charging during observations, the samples were prepared by depositing roughly 50 mg of the material onto an aluminum stud that was covered with conductive adhesive carbon tape. The sample was then coated with Rh-Pd for one minute. Secondary electrons for high vacuum (ETD) were used to perform imaging at an accelerating voltage of 30 kV under high-vacuum circumstances.[31]

Ultimate analysis, humidity and ash content

The ultimate analysis of PGP was carried out using a CHNS-O elemental analyzer (Model Thermo Finnigan Flash EA 1112) according to ASTM D 5373-02. This analysis provided the percentages of carbon, nitrogen, hydrogen, and sulfur. The oxygen content was determined by mass balance, calculated as the difference between 100% and the sum of the other elements' percentages.

Boehm titration

The Boehm titration method was used to determine functional groups on the PGP surface.[32] About 1 g of PGP adsorbent was shaken, separately, with 50 mL of 0.1M solutions of NaOH, 0.1M $NaHCO_3$, 0.05M Na_2CO_3 and 0.1M $NaOC_2H$ at room temperature for 72 h. The suspensions were decanted and filtered, then titrated with 0.1M solution of HCl. The basicity of the adsorbent was determined by a similar procedure. The sample was contacted with 0.1 M of HCl and the titration was done using 0.1M NaOH. The concentration of acidic sites on the adsorbent was calculated by considering that $NaHCO_3$ neutralizes carboxylic groups, Na_2CO_3 neutralizes carboxylic and lactonic groups, $NaOC_2H_5$ neutralizes carboxylic, lactonic, phenolic and carbonyls groups.

Point of zero charge (pH_{pzc})

The point of zero charge (pH_{pzc}) of the PGP adsorbent was determined by adding 0.15 g of PGP adsorbent to 50 mL of 0.01N solution of NaCl whose initial pH was adjusted between 2 and 12 with NaOH or HCl. The containers were stirred for 48 h. Then the samples were filtered and the pH was measured. The intersection of the curve pH_{final} versus $pH_{initial}$ and the bisector gives the value of pH_{pzc}.

FTIR spectrum analysis

The FT-IR spectrum of the adsorbent was recorded in a Nicolet IR200 Model Infrared Spectrophotometer, equipped with a DTGS detector, in the spectrum range of 7800-375 cm^{-1} to determine the functional groups of the samples used.

Adsorption procedure

Effect of pH

The effect of pH on the quantity of adsorbed dye was studied as follows: in 250 mL Erlenmeyer flasks, each containing 200 mL of dye solution at a concentration of 100 mg/L, the initial pH was adjusted to values from 2 to 10 by adding HCl or NaOH (0.01 N) and measured by a Schott pH meter (CG 841 model). To each solution, the same mass of pomegranate peels (0.25 g) was added. The mixtures were allowed to stand for one hour, a time sufficiently long to reach equilibrium. Afterward, the

solutions were filtered, and analysed. The adsorbed quantity was then calculated using Equation (1):

$$q_e = \frac{C_0 - C_e}{m}.V \quad (1)$$

where q_e is the amount of VB adsorbed per gram of PGP (mg/g), C_0 is the initial VB concentration (mg/L), C e is the concentration of VB remained in the solution (mg/L), V is the volume of VB solution (L) and m is the mass of PGP (g).

Adsorption kinetics

To determine the adsorption kinetics of the dye onto pomegranate peels, the following steps were followed: in an Erlenmeyer flask, 2 L of a solution containing the dye at a concentration of 100 mg/L at initial pH 6 was brought into contact with 2 g of pomegranate peels. The resulting mixture was stirred using a mechanical stirrer at a speed of 400 rpm and a temperature of 25 ± 1 °C.

The initial pH of the solution was maintained at 6, and the samples were taken at well-defined time intervals to track the residual dye concentration in the solution over time. The quantity adsorbed at time t was calculated using the following relation:

$$q_t = \frac{(C_0 - C_t)}{m} V \quad (2)$$

where C_0 is the initial concentration of dye in the solution, C_t is the concentration of dye in the solution at time t and m is the mass of PGP (g). Two kinetic parameters were selected for this study: the initial dye concentration and the particle size.

Adsorption isotherms

Adsorption isotherm experiments were carried out at different temperatures (25, 30, 40 and 50 °C) by shaking 0.25 g of PGP adsorbent with 200 mL sample of VB solution of different initial concentrations ranging from 10 to 100 mg/L at optimum pH (=6). The amount of VB adsorbed onto raw pomegranate peel, q_e (mg/g), was calculated using Equation (1).

RESULTS AND DISCUSSION

Physical and chemical characterization of PGP

The N_2 adsorption-desorption isotherms at 77 K of raw PGP are shown in Figure 2. The isotherm is of type III according to the International Union of Pure and Applied Chemistry classification. It is evident that the adsorbent-adsorbate attraction is weak and the adsorption is in multilayer. The BET surface area of the raw PGP waste is <1 m^2/g.

The SEM images of raw PGP are shown in Figure 3.

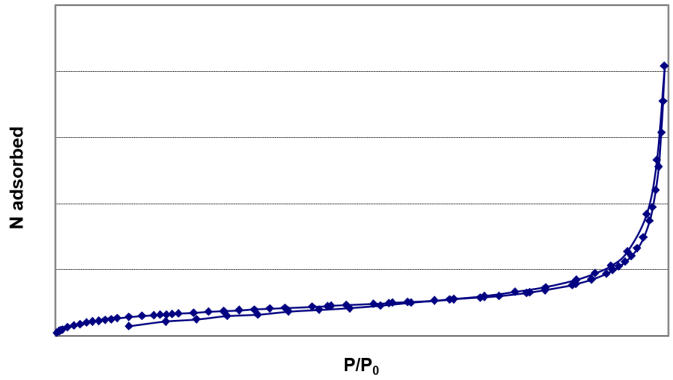

Figure 2: Nitrogen adsorption isotherms of the PGP

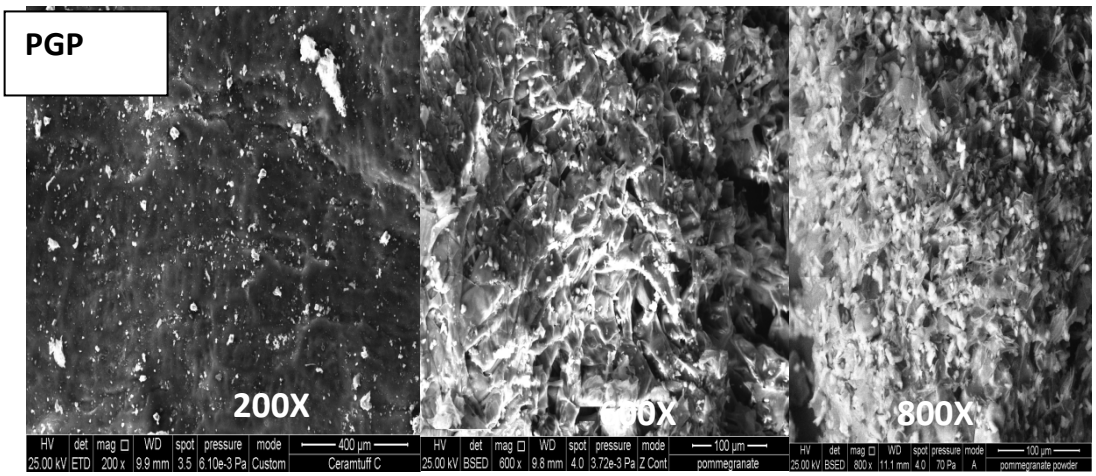

Figure 3: SEM micrographs of pomegranate peels

Table 1
Physical and chemical properties of raw PGP

Parameters	Experimental values
C (%)	43.13
O (%)	48.15
H (%)	7.17
S (%)	0.89
N (%)	0.66
Carboxyl content (meq/g)	0.50
Carbonyl content (meq/g)	1.10
Phenol content (meq/g)	1.80
Total acidic groups (meq/g)	3.40
Total basic groups (meq/g)	0.50
pH_{pzc}	4.70
pH	4.16
Moisture content (%)	8.12
Ash content (%)	9.68
Apparent density (g/cm^3)	0.38
Specific surface area (m^2/g)	<1 m^2/g

The micrographs reveal a rigid, fibrous plant structure. The surface appears smooth and free from pores.

The elemental analysis of the PGP adsorbent showed that the main constituents are 43.13% carbon, 48.15% oxygen, 7.17% hydrogen, 0.66% nitrogen and 0.89% sulfur.

This composition is comparable to Turkish pomegranate peels, reported to have 43.94% carbon, 4.73% hydrogen,1.23% nitrogen and 0.55% sulfur.[33] Moisture content and ash content were 8.12% and 9.68%, respectively. The physical and chemical characterization of PGP were obtained as described by Bedoui and Souissi-Najar.[34]

The mineral species present in the PGP were also determined in the ashes obtained at low temperature. The crystalline species of PGP ashes were identified through X-ray diffraction. The XRD spectrum (figure not shown here) revealed that the main mineral phases are lime (free CaO), MgO, larnite ($2CaO•SiO_2$), calcium carbonate ($CaCO_3$), quartz (SiO_2), brown millerite ($4CaO_4•Al_2Fe_2O_6$), and calcium aluminosilicate ($2CaO•Al2O_3•SiO_2$), within the 2θ range of 25-35°.[29]

Physico-chemical properties of the adsorbent were also determined. The pH of the adsorbent was found to be 4.16. This pH value informs about the acidic nature of raw PGP. Moisture and ash contents were, respectively, 8.12% and 9.68%. The pH_{pzc} was found to be equal to 4.7. Consequently, the surface is positively charged at pH values below the pH_{pzc} and negatively charged at higher pH values.

The surface chemistry of the samples was analysed by the Boehm method. As shown in Table 1, the concentration of the acidic functional groups is more significant on the surface of the PGP adsorbent (3.4 meq/g).

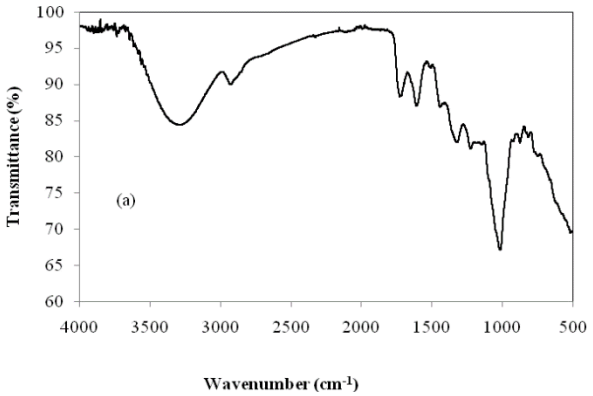

Figure 4: Infrared spectrum of raw PGP

Table 2
Frequencies of different PGP surface functional groups

Frequency (cm^{-1})	Band
1029.18/875.7	(C-O)
1322.65/748.7	C-H aliphatic: ($-CH_3$) or ($-CH_2$)
1607.21	(C=C) and (C=O)
1713.53	(C=O) carboxylic acid, Acetate, ketone, aldehyde
2941	(C-H) aliphatic, ($-CH_3$) or ($-CH_2$)
3292.68	(O-H) of phenolic and carboxylic acid

The FTIR spectrum of PGP is shown in Figure 4. The corresponding absorption bands have been assigned to functional groups using data from the literature.[34,35] The frequencies of different pomegranate surface functional groups are given in Table 2. The absorption bands were attributed to the corresponding groups.[35] The peaks at 1322.65 cm^{-1} and 1029.18 cm^{-1} were assigned to (C-O) groups of carboxylic acid, phenolic, ether and ester groups. The band located at 1607.21 cm^{-1} indicates the stretching vibration of (C=O) and (C=C). The peak around 1713.53 cm^{-1} represents C=O groups (carboxylic acid, acetate groups COO, ketone, aldehyde). The band located at about 2941 cm^{-1} corresponds to the stretching vibration of aliphatic C-H groups. The band at about 3292.68 cm^{-1} can be attributed to the O–H stretching mode of hydroxyl functional groups, and phenolic and carboxylic groups.

These results agree with the surface functional groups determined by the Boehm titration method. Therefore, the study confirmed the presence of hydroxyl groups on the surface of PGP, which are the main effective sites for adsorption.[34,36]

Adsorption studies

Adsorption as a function of the dye solution pH

The initial solution pH is one of the most important parameters influencing any sorption process. It affects the adsorbent surface charge and the degree of ionization. To study the influence of pH on the adsorption capacity of PGP samples for Victoria blue, experiments were performed using various initial solution pH values, from 2 to 10 (Fig. 5).

Biosorption potential of PGP for VB increases with the increase in solution pH. The uptake of VB onto the PGP sample at pH 6 and 8 exhibited 120 mg/g and 115 mg/g, respectively. It decreases to 74.5 at pH 10. However, the percent uptake is much less at pH 2, showing only 20 mg/g adsorption capacity (Fig. 5). The optimum pH for VB biosorption was found to be 6 and it was used for further studies. VB is a cationic dye, which is positively charged in aqueous solution.[37] Therefore, the degree of its sorption onto the PGP surface is primarily dependent on the surface charge on the biosorbent, which in turn is influenced by the solution pH. In effect, the surface of the adsorbent is positively charged for pH<4.7 and it becomes negatively charged for pH value above 4.7. Therefore, for pH values <4.7, the adsorption is unfavourable because of repulsive electrostatic interactions between VB and positively charged functional groups of PGP. The maximum adsorption capacity of VB occurs at a pH above the pH_{pzc} value when the surface of the adsorbent is negatively charged. Consequently, the optimum pH was found to be 6. The other adsorption experiments were performed at this pH value.

Adsorption as a function of initial dye concentration and contact time

To study the influence of the initial concentration of the dye on the adsorption kinetics, the initial concentration was varied as follows: 40, 60, 80 and 100 mg/L at pH = 6. The results of this study are shown in Figure 6. The adsorption capacity of VB increased from 31.08 mg/g to 113.51 mg/g as the initial concentration increased from 40 mg/L to 100 mg/L, until it reached a constant value where no more dye could be adsorbed (the equilibrium point = 20 min). Initially, the number of available active sites is higher and the transfer force of the solute to the pomegranate peel is greater. This is why the solute reaches the adsorption sites easily. After a point, the adsorption kinetics slows down. This can be explained by the accumulation of dye molecules at the available sites, which makes their displacements more difficult. Other authors found similar results.[38,39]

Adsorption as a function of temperature

The study of the temperature dependence of adsorption reactions gives important information

about the enthalpy change through adsorption. The removal efficiency of pomegranate peel for VB under varying temperature was studied by carrying out a series of isotherms at 25, 30, 40 and 50 °C. Figure 7 presents the adsorption capacity of PGP for VB as a function of time at different temperatures.

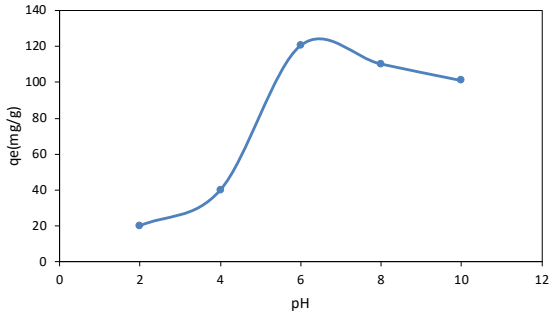

Figure 5: Effect of initial pH on VB adsorption onto PGP (T = 30 °C, C_0 = 100 mg/L, adsorbent dose = 0.1 g, particle size ≤0.63 mm)

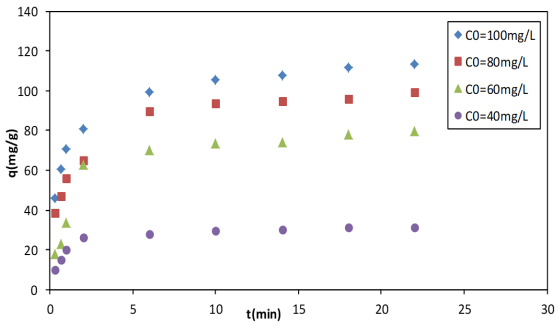

Figure 6: Effect of initial concentration on VB adsorption on PGP adsorbent (T = 30 °C, pH = 6, adsorbent dose = 0.1 g, particle size ≤0.63 mm)

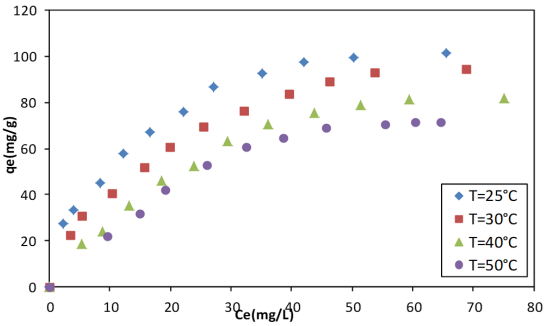

Figure 7: Effect of temperature on the adsorption capacity of VB on PGP adsorbent (C_0 = 100 mg/L, pH = 6, adsorbent dose = 0.1 g, particle size ≤0.63 mm)

After examining the dye removal efficiency, it was determined that the increase in temperature led to a decrease in the adsorption capacity, which reveals that the process is exothermic. The effect of temperature is quite common, increasing the temperature must increase the mobility of the large dye cation.[40] On the other hand, increasing temperature may cause the destruction of the pomegranate structure and probably decrease the surface of active sites, subsequently affecting the adsorption capacity. Thus, the thickness of the boundary layer decreases due to increased tendency of the VB molecules to get away from the adsorbent surface to the solution phase, which results in lower adsorption capacity.[41] Deniz *et al.*[42] reported comparable results for the adsorption of Basic Red 46 onto princess tree leaf.

Eventually, the adsorption process does not significantly change over 30 °C and continuous curves indicate biosorbent surface saturation with dye molecules, which occupied all the active sites.[42] The exothermic nature of VB adsorption on pomegranate peel will be confirmed subsequently during the thermodynamic study.

Adsorption as a function of absorbent particle size

The effect of varying the biosorbent particle size on the adsorption capacity is shown in Figure 8. Results show that the smaller the particle size (0.63 mm), the higher the VB adsorption capacity (113.51 mg/g). This result can be due to the increase in the accessible surface area, which provided more available sorption sites. Ponnusami *et al.*[43] reported similar findings for adsorbent particle size on methylene blue adsorption. Also, in the case of the biosorption of Acid Orange 52 onto *Paulownia tomentosa* leaf powder,[37] the results showed that higher dye removal was achieved by smaller particles. Actually, an increase in the particle size from 0.63–0.125 to 0.125-0.25 mm led

to an increase in the adsorption capacity from 20.12 to 21.66 mg/g for the biosorbent. Maximum adsorption occurred with the biosorbent size >0.125 mm, as compared to particles having larger size.

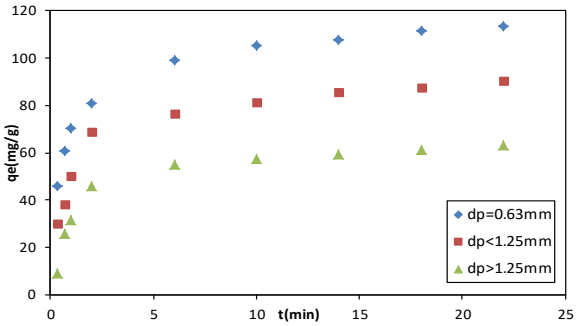

Figure 8: Effect of particle size on the adsorption capacity of VB on PGP adsorbent (C_0 = 100 mg/L, T = 30 °C, pH = 6, adsorbent dose = 0.1 g)

Biosorption isotherms

The purpose of the adsorption isotherms is to describe equilibrium and interaction between adsorbate and adsorbent. The equilibrium isotherm of adsorption is established between the adsorbate concentration removed from the solution per gram of adsorbent and the residual amount of adsorbate in solution.[44,45] The values of the adsorption isotherm constants quantify the affinity and the surface properties of PGP towards VB. Three isotherm models were selected in this study: Langmuir, Freundlich and Temkin isotherms, and will be discussed below.

Langmuir isotherm

The Langmuir isotherm[46] assumes that the adsorption process takes place at specific homogeneous sites on the adsorbent surface and that once a dye molecule occupies a site, no further adsorption can take place at that site. The model assumes uniform energies of adsorption onto the surface and there is no interaction between the adsorbed molecules as a result, adsorption occurs as monolayer. The simple form of the Langmuir equation is given as:

$$q_e = \frac{q_\infty K_L C_e}{1+K_L C_e} \quad (3)$$

The linearized form of the Langmuir isotherm equations is:

$$\frac{C_e}{q_e} = \frac{1}{q_\infty K_L} + \frac{C_e}{q_\infty} \quad (4)$$

where q_e is dye concentration adsorbed at equilibrium (mg/g), q_∞ is the maximum monolayer capacity of the adsorbent (mg/g), K_L is the adsorption constant (L/mg) and C_e is the equilibrium dye concentration in solution (mg/L). According to Equation (4), a plot of $1/q_e$ versus $1/C_e$ should be a straight line with a slope $1/q_\infty$ and intercept $1/q_\infty K_L$ when adsorption follows the Langmuir equation.[47]

The maximum monolayer capacity q_∞ is 101.6 mg/g at T = 25 °C. The Langmuir constants are given in Table 3. For different studied temperatures, the regression coefficients R^2 showed that the Langmuir isotherm fitted well with the experimental data. The Langmuir maximum adsorption capacity $q\infty$ decreases from 101.6 mg/g to 71.42 mg/g as the temperature increases from 25 to 50 °C; this can be explained by the fact that VB adsorption is an exothermic process.

In order to determine if the adsorption process is favorable or unfavorable, a dimensionless constant separation factor R_L is defined by the following equation:

$$R_L = \frac{1}{1+K_L C_e} \quad (5)$$

The R_L value indicates whether the type of isotherm is favourable ($0 < R_L < 1$), unfavorable ($R_L > 1$), linear ($R_L = 1$), or irreversible ($R_L = 0$).[17,48] In this study, R_L was found to be in the range of 0.889–0.998 for initial dye concentration values ranging from 40 to 100 mg/L, which is an indication of favourable adsorption of VB on the adsorbent.

Freundlich isotherm

The Freundlich isotherm model suggests that adsorption occurs as multilayer because of non-uniform distribution of active sites on heterogeneous surfaces and there is interaction between the adsorbed molecules. It also assumes that the stronger binding sites are initially occupied

and that the binding energies decrease with increasing site occupation. The simple form of the Freundlich model is defined as:[18]

$$q_e = K_f C_e^{1/n_f} \quad (6)$$

The linearized form of Freundlich isotherm model equations is:

$$Ln\ q_e = Ln\ K_f + \frac{1}{n_f} Ln\ C_e \quad (7)$$

where K_f is the Freundlich constant and n gives information about bond energies between metal ions and the adsorbent. A plot of Ln q_e versus Ln C_e is a straight line with a slope 1/n and intercept Ln K_f. Freundlich parameters are given in Table 3. The value of 1/n ranging between 0 and 1 is a measure of adsorption intensity or surface heterogeneity. It becomes more heterogeneous as its value gets closer to zero, and a value for 1/n below one indicates a normal Langmuir isotherm.

Considering the experimental data for the equilibrium adsorption of VB on the PGP biosorbent, the correlation coefficients obtained for different temperatures range from 0.839 to 0.994, and the 1/n values were seen to be less than 1, which indicates that the biosorption of VB onto PGP is favorable.

Temkin isotherm

The Temkin isotherm assumes that during the adsorption process, beside adsorbent sites saturation, the adsorption energy decreases linearly rather than decreasing exponentially. Furthermore, this isotherm contains a factor explicitly taking into account the adsorbent–adsorbate interactions. The equation for Temkin isotherm model is the following:[49]

$$q_e = BLn\ (A_T C_e) \quad (8)$$

where C_e is the equilibrium VB concentration in the solution (mg/L), q_e is the equilibrium VB concentration on the adsorbent (mg/g); B = RT/b, b is the Temkin isotherm constant and A_T is the Temkin isotherm parameters, related to the equilibrium binding constant (L/mg) and the heat of adsorption, respectively.

The Temkin model is presented in linear form by the following equation:

$$q_e = BLn\ A_T + BLn\ C_e \quad (9)$$

The Temkin parameters are presented in Table 3. The regression value R^2 obtained for different temperatures are between 0.972 and 0.98.

Figure 9 illustrates a comparison between the three isotherm models used in this study: Langmuir, Freundlich and Temkin for different temperatures (25, 30, 40 and 50 °C). The adsorption of VB onto PGP is best described by the Langmuir model. This model's fit to experimental data, particularly at high temperatures (40 and 50 °C), is superior to that of the Freundlich and Temkin models. This suggests that VB adsorption occurs primarily as a monolayer on a relatively homogeneous surface with a finite number of identical active sites. The validity of the Langmuir hypothesis is confirmed by the surface characterization results. FTIR analysis revealed the presence of oxygenated functional groups, such as hydroxyl (–OH), carboxyl (–COOH), and carbonyl (C=O) groups, which constitute active adsorption sites. Furthermore, Boehm titration confirmed the predominance of acidic groups, indicating a surface chemistry favorable to the binding of cationic dyes. Furthermore, the pH_{pzc} value provides information on the adsorption mechanism. At pH values above pH_{pzc}, the PGP surface becomes negatively charged, strengthening the electrostatic attraction with the positively charged VB molecules. Therefore, electrostatic interactions are likely the primary driving force of the adsorption process, complemented by possible hydrogen bonding and π–π interactions.

Table 3
Langmuir, Freundlich and Temkin isotherm model constants for adsorption of VB onto raw PGP adsorbent

	Langmuir model			Freundlich model			Temkin model		
T (°C)	q_{exp} (mg/g)	K_L	R^2	K_f	$1/n_f$	R^2	A_T	B	R^2
25	120.48	0.09	0.94	19.196	0.249	0.98	0.96	25.28	0.97
30	120.48	0.06	0.99	13.105	0.496	0.98	0.56	26.20	0.98
40	121.95	0.033	0.95	7.188	0.608	0.96	0.31	27.69	0.97
50	114.94	0.029	0.99	6.521	0.605	0.93	0.24	27.45	0.97

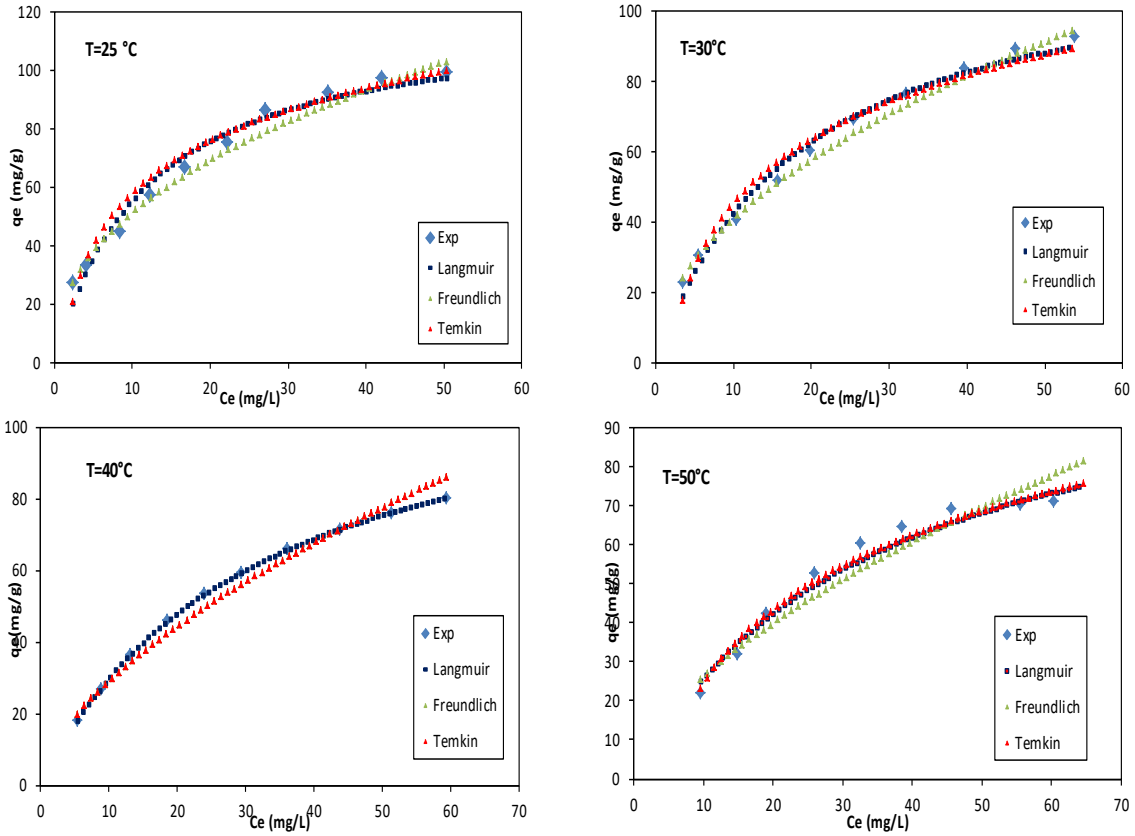

Figure 9: Plots of Langmuir isotherm, Freundlich isotherm, Temkin isotherm, and experimental data of adsorption capacity of PGP for VB at different temperatures (pH = 6; particle size ≤ 0.63 mm)

Overall, the agreement between isotherm modeling and physicochemical characterization suggests that VB adsorption onto PGP is governed by the formation of a monolayer at homogeneous active sites, primarily driven by electrostatic attraction.

Adsorption kinetics

Pseudo first and second order models

Kinetic models are used to understand the mechanism of the adsorption process and the behavior of the adsorbent. In the present study, the adsorption data were analyzed using three kinetic models, the pseudo first order, pseudo second order kinetic and the intraparticle diffusion models.

The pseudo first order kinetic model equation[50] describes adsorption in liquid-solid systems. Lagergren's first-order reaction model is expressed in linear form as Equation (10):

$$\frac{dq_t}{dt} = K_1(q_e - q_t) \quad (10)$$

where K_1 is the rate constant of the first order kinetic model (min^{-1}), q_t and q_e are the amount of VB dye adsorbed on PGP at equilibrium and at a time t, respectively (mg/g). The linearized form of the pseudo first order model equation is:

$$Ln\ (q_e - q_t) = Ln\ q_e - K_1 t \quad (11)$$

The slopes and intercept of Ln (q_e - q_t) versus t plot were used to calculate K_1 and q_e (Fig. 10a).

The adsorption data were also analyzed in terms of the pseudo second order mechanism, described by Ho and McKay.[51] The pseudo second order model is based on chemisorption, and is expressed as:

$$\frac{dq_t}{dt} = K_2(q_e - q_t)^2 \quad (12)$$

where K_2 is the rate constant of the second-order kinetic model (g/mg.min), q_t and q_e are the amount of VB dye adsorbed on PGP at equilibrium and at a time t, respectively (mg/g). The linearized form of the pseudo second order model is:

$$\frac{t}{q_t} = \frac{1}{K_2 q_e^2} + \frac{1}{q_e} t \quad (13)$$

The plot of t/q_t against t should give a linear relationship with a slope of $1/q_e$ and an intercept of $1 / K_2 q_e^2$ (Fig. 10 b).

The linear forms of the pseudo-first order and pseudo-second order kinetic models for VB adsorption onto PGP at 30 °C are shown in Figure

10, and the kinetic parameters and correlation coefficients are summarized in Table 4.

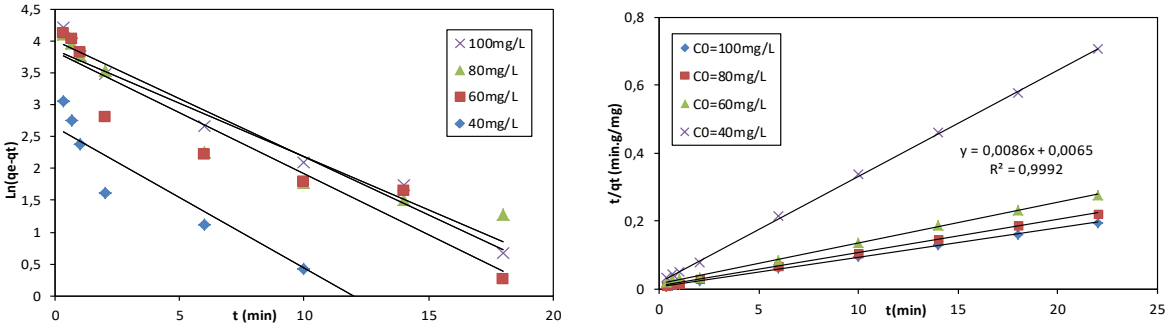

a) b)

Figure 10: Linear kinetic plots for VB dye adsorption on raw PGP adsorbent: (a) pseudo first-order model and (b) pseudo second-order model (pH = 6, particle size <0.63 mm, T = 30 °C)

Table 4
Pseudo first order, Pseudo second order constants and model correlations coefficients

	Pseudo-first order				Pseudo-second order		
C_0 (mg/L)	q_{exp} (mg/g)	K_1	q_e (mg/g)	R^2	K_2	q_e (mg/g)	R^2
40	31.08	0.22	14.23	0.92	0.04	32.05	0.99
60	79.42	0.19	46.25	0.91	0.01	83.33	0.99
80	99.45	0.16	47.29	0.91	0.01	102.04	0.99
100	113.51	0.18	54.81	0.98	0.01	116.27	0.99

The adsorption process is primarily governed by the presence of functional groups on the surface of the adsorbent, such as hydroxyl (–OH), carboxyl (–COOH), carbonyl (C=O), and Fe–O groups, which interact with the dye molecules through electrostatic attraction, hydrogen bonding, and π–π interactions. For different initial VB concentrations, the correlation coefficients of the pseudo-second-order model are the highest, and the calculated equilibrium adsorption capacities are closest to the experimental data, suggesting that adsorption involves both physical and chemical interactions. This is corroborated by the thermodynamic parameters, in particular the value of ΔH° (−34.48 kJ/mol), which indicates a mixed adsorption mechanism. Thus, the pseudo-second-order kinetic model provides a better description of the adsorption process than the pseudo-first-order model. This suggests that the rate-limiting step may involve surface interactions, including valence forces through sharing or exchange of electrons, without excluding the contribution of physical interactions. Similar results have been reported for the sorption of BG4 on clayey soil.[52] As shown in Table 4, the rate constant K_2 decreases with increasing initial dye concentration. This behavior can be attributed to the increased competition for active adsorption sites at higher concentrations, leading to lower adsorption rates. Comparable results have been reported for the adsorption of BG on sawdust biosorbent[53] and deoiled soya.[54]

Intraparticle diffusion model

To identify the diffusion mechanism of VB on PGP, the Weber–Morris intraparticle diffusion model was employed. Most adsorption processes consist of a number of steps, including surface diffusion and intraparticle diffusion. The intraparticle diffusion approach proposed by Weber and Morris is described by:[55]

$$q_t = K_P t^{1/2} \quad (14)$$

where q_t is the amount of dye adsorbed at time t (mg/g), C is the intercept, and k_p is the intraparticle diffusion rate constant (mg/g·min$^{0.5}$), which can be calculated from the slope of the linear plot of q_t versus $t^{1/2}$, as shown in Figure 11. The values of K_p and the intercept obtained at different initial concentration of the dye are listed in Table 5.

If the biosorption mechanism follows the intraparticle diffusion process, the plot of q_t versus $t^{0.5}$ should be a straight line with a slope K_i and intercept C. However, if the data shows multi-linear plots, then the process is controlled by two or more steps. As shown in Figure 11, the plot has two portions, an initial curved portion and a second linear portion, suggesting that the adsorption

process has two phases. The curve of the first portion of the plot is the result of external surface adsorption, indicating a boundary layer effect, while the linear portion reflects intraparticle or pore diffusion. For different concentrations, the linear portions of the curves do not pass through the origin, signifying that intraparticle diffusion is not the only rate-limiting step.[50,56] Besides, the intercept value C decreases with increasing initial VB concentration, which is indicative of a decrease in the thickness of the boundary layer and its effect on adsorption. The values of K_p obtained at different initial concentration of the dye are listed in Table 5.

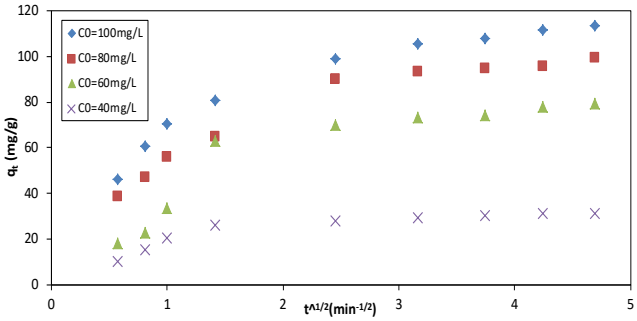

Figure 11: The intraparticle diffusion kinetic model for adsorption of VB on PGP (pH = 6, particle size <0.63 mm, T = 30 °C)

Table 5
Kinetic parameters for the intraparticle diffusion model

	First portion			Second portion		
C_0 (mg/L)	K_{p1}	C	R^2	K_{p2}	C	R^2
40	19.06	-0.17	0.98	1.43	24.80	0.93
60	55.28	-18.17	0.95	4.14	59.92	0.97
80	31.59	21.71	0.97	3.79	80.86	0.95
100	40.69	25.85	0.95	6.32	84.37	0.98

Adsorbent regeneration and reusability

In the present study, no regeneration or reuse tests were performed for VB. However, regeneration experiments were previously conducted on this adsorbent in a related study using MB as a model dye. The adsorbent demonstrated good stability and maintained high adsorption efficiency over several cycles. Since both MB and VB are cationic dyes, these results suggest that the prepared biosorbent might exhibit good reusability for VB as well, although further specific experiments are needed to confirm this behavior.

Biosorption thermodynamics

To evaluate the spontaneity of the adsorption process, the values of thermodynamic parameters, such as the Gibbs free energy change (ΔG°), enthalpy change (ΔH°), and entropy change (ΔS°), were calculated by the following equations:

$$\Delta G^0 = \Delta H^0 - T\Delta S^0 \quad (15)$$

$$\Delta G^0 = -RT\ Ln\ (K_L) \quad (16)$$

where K_L, obtained from the Langmuir isotherm equation and R and T are gas constant (8.314 J=mol K) and absolute temperature (Kelvin) respectively. ΔH° and ΔS° values of the biosorption process were calculated from the van't Hoff equation:[36]

$$ln\ K = \frac{-\Delta H}{R}\frac{1}{T} + \frac{\Delta S}{R} \quad (17)$$

The values of ΔH° and ΔS° can be determined from the slope and intercept of the linear plot of In K_L versus 1/T for the adsorption of VB onto PGP at different temperature with the slope (-ΔH°/R) and intercept (ΔS°/R) are found. The values of Gibbs free energy change of the biosorption process can be calculated using K_L at all temperatures. The results are given in Table 6.

Table 6
Thermodynamic parameters of adsorption of VB on PGP

T (K)	ΔG° (J/mol)	ΔH° (J/mol)	ΔS° (J/mol.K)
298	-34680.02	-34480	0.66
303	-34683.31		
313	-34689.89		
323	-34696.47		

The values of thermodynamic parameters are given in Table 6. The negative ΔG° values suggest that the adsorption process is spontaneous.[53] The decrease in the negative values of ΔG° with increasing temperature implies that the adsorption is less favourable at higher temperatures.[57] Besides, the negative value of ΔH° confirm that the adsorption process is exothermic.[58] On the other hand, the positive values of ΔS° indicate increased randomness at the interface during the biosorption of VB onto PGP.[35]

The ΔH° values give information about the forces involved in the sorption process. The energy associated with different physical forces, such as van der Waals forces, is between 4 and 10 kJ/mol, for hydrophobic bond forces it is about 5 kJ/mol, for hydrogen bond forces it ranges from 2 to 40 kJ/mol and for chemical forces the energy is higher than 60 kJ/mol.[59] In this work, ΔH° was found to be -34.48 kJ/mol, which suggests that the forces involved in the sorption process are physical.

Comparative study

The comparison presented in Table 7 highlights significant differences in VB adsorption capacities (q_{max}) depending on the nature of the adsorbent, its processing, and the experimental conditions. Among the materials tested, the raw pomegranate peels used in this study exhibited a relatively high adsorption capacity (120.48 mg/g), surpassing several conventional and economical adsorbents, such as clay (5.37 mg/g) and unexpanded perlite (3.68 mg/g). Comparable performance was observed for other raw biomasses, such as *Zizyphus oenoplia* seeds (119 mg/g), confirming the strong potential of untreated agricultural waste.

However, some materials showed superior capacities, notably palm petioles (440 mg/g) and zinc oxide nanoparticles (163 mg/g), which can be attributed to their surface properties or modification effects. In contrast, some modified or activated adsorbents, such as activated carbon composites, exhibited relatively low q_{max} values (≈1.65–1.98 mg/g), likely due to differences in experimental conditions, initial dye concentration, or pore accessibility. Overall, this comparison demonstrates that PGP, even without chemical treatment, can be a highly effective adsorbent for removing VB. Its performance, combined with its low cost, abundance, and environmentally friendly nature, makes it a promising candidate for sustainable wastewater treatment. Notably, only a few studies have specifically addressed VB removal, which highlights the contribution of the present study in advancing knowledge with valuable data in the field of dye biosorption.

Table 7
Comparison of adsorption capacities of different adsorbents for the removal of VB

Adsorbent	Adsorbent treatment	Q_{max} (mg/g)	C_0 (mg/L)	pH	T (°C)	Refs.
Pomegranate peels	Raw	120.48	40-100	6	30	This study
Zizyphus oenoplia seed	Raw	119	-	5	30	[14]
Petiole palm tree	Raw	440	10-50	4	20	[15]
Clay	Raw	5.37	3-30	2-11	30	[60]
Commercial activated carbon	Activated	33.64	10-100			
Titanium dioxide nano bio-adsorbent	Modified	83.3	30-80	6	25	[61]
Activated carbon	Activated	1.98	4-20	5	30	[58]
Activated carbon/Ba		1.65				
Activated carbon/Ba/alginate beads		1.94				
Zinc oxide nanoparticles	Modified	163	-	6	27	[38]
Unexpanded perlite	Raw	3.68	_	6	30	[36]
Pomegranate peels	Raw	1.46	25	NA	45	[62]

CONCLUSION

This study demonstrates the effectiveness of raw pomegranate peel (PGP) as a low-cost, eco-friendly, and sustainable biosorbent for the removal of Victoria Blue dye from aqueous solutions. The physicochemical characterization revealed that PGP possesses a fibrous structure with predominantly acidic functional groups, although it has a relatively low surface area (<1 m^2/g). Despite this, PGP exhibited a high adsorption capacity of 120.48 mg/g under optimal conditions (pH 6, 0.1 g biosorbent dose, particle size ≤ 0.63 mm, 100 mg/L dye concentration, and 30 °C).

Adsorption equilibrium data were best described by the Langmuir isotherm model, indicating monolayer adsorption on a homogeneous surface. Kinetic studies revealed that the biosorption process followed a pseudo-second-order model, suggesting that chemisorption is the dominant mechanism. Furthermore, thermodynamic parameters confirmed the exothermic nature of the process.

Overall, the findings highlight the potential of pomegranate peel waste as an efficient and sustainable biosorbent for dye removal in wastewater treatment applications. Its abundant availability and high adsorption performance make it a promising alternative to conventional treatment methods in addressing dye-contaminated effluents.

REFERENCES

[1] N. N. Same, A. O. Yakub, D. Chaulagain, J. Park, A. B. Owolabi *et al*., *Energ. Nexus*, **18**, 100408 (2025), https://doi.org/10.1016/j.nexus.2025.100408

[2] A. Addo and F. Kemausuor, *Ghana J. Technol*., **5**, 29 (2021)

[3] S. Nawaz, F. Jamil, P. Akhter, M. Hussain, H. Jang *et al*., *J. Phys. Energ*., **5**, 1 (2023), https://doi.org/10.1088/2515-7655/aca5b4

[4] S. Başakçılardan Kabakcı and S. S. Baran, *Waste Manag*., **100**, 259 (2019), https://doi.org/10.1016/j.wasman.2019.09.021

[5] B. Ligas, J. Warchoł and D. Skrzypczak, *Waste Biomass Valor*., **13**, 1913 (2022), https://doi.org/10.1007/s12649-021-01639-z

[6] O. J. Al-Sareji, M. Meiczinger and R. A. Al-Juboori, *Sci. Rep*., **13**, 1 (2023), https://doi.org/10.1038/s41598-023-38821-3

[7] A. Ashfaq, R. Nadeem and S. Bibi, *Water*, **13**, 3344 (2021), https://doi.org/10.3390/w13233344

[8] A. Bourafa, E. Berrich, M. Belhachemi, S. Jellali and M. Jeguirim, *Biomass Conv. Bioref*., **14**, 20385 (2024), https://doi.org/10.1007/s13399-023-04225-6

[9] K. Ravichandran and R. Paramasivam, *Biomass Conv. Bioref*. (2025), https://doi.org/10.1007/s13399-025-06511-x

[10] A. Bedoui, S. Souissi-Najar, S. S. Idris Abd Rahman and A. Ouederni, *C. R. Chim*., **15**, 1 (2021), https://doi.org/10.1016/j.crci.2015.07.016

[11] A. Bedoui, H. Nouri, M. Boutaieb, R. Ghouil, B. Ledesma *et al*., *C. R. Chim*., **15**, 1060 (2024), https://doi.org/10.5802/crchim.366

[12] D. Khodaei, C. Álvarez and A. M. Mullen, *Polymers*, **13**, 2561 (2021), https://doi.org/10.3390/polym13152561

[13] Y. Zhang, D. Wu, Y. Su and B. Xie, *Bioresour. Technol*., **330**, 124987 (2021), https://doi.org/10.1016/j.biortech.2021.124987

[14] R. Tamilarasan, V. Sureshkumar and M. Kumar, in *Proc. 2016 International Conference on Emerging Trends in Engineering, Technology and Science (ICETETS)*, Pudukkottai, India, 2016, pp. 1-8, https://doi.org/10.1109/ICETETS.2016.7603126

[15] S. Jmai, S. Guiza, S. Jellali, M. Bagane and M. Jeguirim, *C. R. Chim*., **15**, 1 (2016)

[16] S. Ben-Ali, I. Jaouali, S. Souissi-Najar and A. Ouederni, *J. Clean Prod*., **142**, 3809 (2017), https://doi.org/10.1016/j.jclepro.2016.10.081

[17] S. Banerjee, G. C. Sharma and R. K. Gautam, *J. Mol. Liq*., **213**, 162 (2016), https://doi.org/10.1016/j.molliq.2015.11.011

[18] H. Shayesteh, A. Rahbar-Kelishami and R. Norouzbeigi, *Desal. Water Treat*., **57**, 12822 (2016), https://doi.org/10.1080/19443994.2015.1054315

[19] M. Rauf, I. Shehadeh, A. Ahmed and A. Alzamly, *World Acad. Sci. Eng. Technol*., **31** (2009)

[20] J. Wu, C. Yang, H. Zhao, J. Shi, Z. Liu *et al*., *Environ. Sci. Pollut. Res*., **30**, 26914 (2023), https://doi.org/10.1007/s11356-022-24130-1

[21] L. Zhou, J. Jin, Z. Liu, X. Liang and C. Shang, *J. Hazard. Mater*., **185**, 1045 (2011), https://doi.org/10.1016/j.jhazmat.2010.10.012

[22] J. Song, W. Zou, Y. Bian, F. Su and R. Han, *Desalination*, **265**, 119 (2011), https://doi.org/10.1016/j.desal.2010.07.041

[23] S. Chowdhury, R. Mishra, P. Saha and P. Kushwaha, *Desalination*, **265**, 159 (2011), https://doi.org/10.1016/j.desal.2010.07.047

[24] N. Soudani, S. Souissi-Najar and A. Ouederni, *Chin. J. Chem. Eng*., **21**, 1425 (2013), https://doi.org/10.1016/S1004-9541(13)60638-2

[25] O. Fasakin, J. K. Dangbegnon, D. Y. Momodu, M. J. Madito, K. O. Oyedotun *et al*., *Electrochim. Acta*, **262**, 187 (2018), https://doi.org/10.1016/j.electacta.2018.01.028

[26] R. Fang, H. Huang and J. Ji, *Chem. Eng. J*., **334**, 2050 (2018), https://doi.org/10.1016/j.cej.2017.11.176

[27] H. Saad, F. Charrier-El Bouhtoury and A. Pizzi, *Ind. Crop. Prod*., **40**, 239 (2012), https://doi.org/10.1016/j.indcrop.2012.02.038

[28] M. E. M. Ali, H. Abdelsalam, N. S. Ammar and H. S. Ibrahim, *J. Mol. Liq.*, **250**, 433 (2018), https://doi.org/10.1016/j.molliq.2017.12.025
[29] S. Ben-Ali, *Adv. Mater. Sci. Eng.* (2021), https://doi.org/10.1155/2021/8840907
[30] S. J. Gregg and K. S. W. Sing, "Adsorption Surface Area and Porosity", 2nd ed., Academic Press, London, 1982
[31] M. Boutaieb, S. Román, B. Ledesma, E. Sabio and M. Guiza *et al.*, *Waste Manag.*, **132**, 115 (2021), https://doi.org/10.1016/j.wasman.2021.07.023
[32] M. Mazet, *Water Res.*, **28**, 1609 (1994), https://doi.org/10.1016/0043-1354(94)90228-3
[33] Ç. Ömeroğlu Ay, A. S. Özcan, Y. Erdoğan and A. Özcan, *Colloids Surf. B*, **100**, 197 (2012), https://doi.org/10.1016/j.colsurfb.2012.05.013
[34] A. Bedoui and S. Souissi-Najar, *E3S Web Conf.*, **697**, 00007 (2026)
[35] F. Güzel, Ö. Aksoy and G. Akkaya, *World Appl. Sci. J.*, **20**, 965 (2012)
[36] O. Demirbaş, M. Alkan and M. Doğan, *Adsorption*, **8**, 341 (2002), https://doi.org/10.1023/A:1021589514766
[37] F. Deniz and S. D. Saygideger, *Bioresour. Technol.*, **101**, 5137 (2010), https://doi.org/10.1016/j.biortech.2010.02.004
[38] N. Kataria, V. K. Garg, M. Jain and K. Kadirvelu, *Adv. Powder Technol.*, **27**, 1180 (2016), https://doi.org/10.1016/j.apt.2016.04.001
[39] E. K. Guechi and O. Hamdaoui, *Desal. Water Treat.*, **57**, 10270 (2016), https://doi.org/10.1080/19443994.2015.1035338
[40] H. M. Asfour, O. A. Fadali, M. M. Nassar and M. S. El-Geundi, *J. Chem. Technol. Biotechnol.*, **35**, 21 (1985), https://doi.org/10.1002/jctb.5040350105
[41] N. Gupta, A. K. Kushwaha and M. C. Chattopadhyaya, *J. Taiwan Inst. Chem. Eng.*, **43**, 604 (2012), https://doi.org/10.1016/j.jtice.2012.01.008
[42] F. Deniz and S. D. Saygideger, *Desalination*, **268**, 6 (2011), https://doi.org/10.1016/j.desal.2010.09.043
[43] V. Ponnusami, V. Gunasekar and S. N. Srivastava, *J. Hazard. Mater.*, **169**, 119 (2009), https://doi.org/10.1016/j.jhazmat.2009.03.066
[44] L. G. Wang and G. B. Yan, *Desalination*, **274**, 81 (2011), https://doi.org/10.1016/j.desal.2011.01.082
[45] M. Ghasemi, S. Mashhadi and M. Asif, *J. Mol. Liq.*, **213**, 317 (2016), https://doi.org/10.1016/j.molliq.2015.09.048
[46] I. Langmuir, *J. Am. Chem. Soc.*, **40**, 1361 (1918), https://doi.org/10.1021/ja02242a004
[47] M. Alkan and M. Doğan, *J. Colloid Interface Sci.*, **243**, 280 (2001), https://doi.org/10.1006/jcis.2001.7796
[48] M. R. R. Kooh, M. K. Dahri and L. B. L. Lim, *Environ. Earth Sci.*, **75**, 783 (2016), https://doi.org/10.1007/s12665-016-5582-9
[49] A. O. Dada, A. Olalekan, A. Olatunya and O. Dada, *J. Appl. Chem.*, **3**, 38 (2012), https://doi.org/10.9790/5736-0313845
[50] S. Venkata Mohan, N. Chandrasekhar Rao and J. Karthikeyan, *J. Hazard. Mater.*, **90**, 189 (2002), https://doi.org/10.1016/S0304-3894(01)00348-X
[51] Y. S. Ho and G. McKay, *Water Res.*, **34**, 735 (2000), https://doi.org/10.1016/S0043-1354(99)00232-8
[52] P. Saha, S. Chowdhury, S. Gupta and I. Kumar, *Chem. Eng. J.*, **165**, 874 (2010), https://doi.org/10.1016/j.cej.2010.10.048
[53] V. S. Mane and P. V. V. Babu, *Desalination*, **273**, 321 (2011), https://doi.org/10.1016/j.desal.2011.01.049
[54] A. Mittal, D. Kaur and J. Mittal, *J. Colloid Interface Sci.*, **326**, 8 (2008), https://doi.org/10.1016/j.jcis.2008.07.005
[55] W. J. Weber and J. C. Morris, *J. Sanit. Eng. Div.*, **89**, 31 (1963), https://doi.org/10.1061/JSEDAI.0000430
[56] X. Yang and B. Al-Duri, *J. Colloid Interface Sci.*, **287**, 25 (2005), https://doi.org/10.1016/j.jcis.2005.01.093
[57] S. Banerjee, G. C. Sharma and R. K. Gautam, *J. Mol. Liq.*, **213**, 162 (2016), https://doi.org/10.1016/j.molliq.2015.11.011
[58] R. Kumar and M. A. Barakat, *Chem. Eng. J.*, **226**, 377 (2013), https://doi.org/10.1016/j.cej.2013.04.063
[59] H. N. Tran, S. J. You and H. P. Chao, *J. Environ. Chem. Eng.*, **4**, 2671 (2016), https://doi.org/10.1016/j.jece.2016.05.009
[60] M. Meenakshisundaram, *J. Chem. Pharm. Res.*, **3**, 584 (2011)
[61] N. Fakhar, W. A. Siddiqi, T. A. Khan and M. F. Siddiqui, *Mater. Res. Express*, **7**, 015077 (2020)
[62] B. Akmese, *BMC Chem.*, **19** (2025), https://doi.org/10.1186/s13065-025-01476-4